



Politecnico
di Bari

Repository Istituzionale dei Prodotti della Ricerca del Politecnico di Bari

Seismic duration effect on damping reduction factor using random vibration theory

This is a pre-print of the following article

Original Citation:

Seismic duration effect on damping reduction factor using random vibration theory / Greco, Rita; Vanzi, Ivo; Lavorato, Davide; Briseghella, Bruno. - In: ENGINEERING STRUCTURES. - ISSN 0141-0296. - STAMPA. - 179:(2019), pp. 296-309. [10.1016/j.engstruct.2018.10.074]

Availability:

This version is available at <http://hdl.handle.net/11589/207145> since: 2021-03-09

Published version

DOI:10.1016/j.engstruct.2018.10.074

Publisher:

Terms of use:

(Article begins on next page)

1 **Seismic duration effect on damping reduction factor using random vibration**

2 **theory**

3 Rita Greco, Ivo Vanzi, Davide Lavorato and Bruno Briseghella

4
5 R. Greco

6 Professor, Technical University of Bari, Via Edoardo Orabona, 4, 70126, Bari, Italy

7 Email: rita.greco@poliba.it

8
9 I. Vanzi

10 Full professor, Department of Engineering and Geology, University of Chieti-Pescara “G. d’Annunzio”, Viale Pindaro
11 42, 65127 Pescara, Italy

12 Email: i.vanzi@unich.it

13
14 D. Lavorato

15 Assistant professor, Dept. of Architecture, Roma Tre University, Largo GB Marzi 10, Rome, Italy

16 Email: davide.lavorato@uniroma3.it

17
18 B. Briseghella (Corresponding author)

19 Full professor, Department of Civil Engineering, University of Fuzhou, Qi Shan Campus of Fuzhou University, 2 Xue
20 Yuan Road, University Town, Fuzhou, Fujian 350108 P. R. China.

21 Email: bruno@fzu.edu.cn

22 23 **Abstract**

24 Damping Reduction Factor plays a key role in scientific literature and Technical Codes, but till now
25 existing formulations present differences and inconsistencies probably because obtained by
26 integration of real recorded events, thus sensitive to specific used data. This paper investigates the
27 relation between damping reduction factor and earthquake duration by means of random vibration
28 theory. A stochastic process, that is non-stationary and filtered, is used to model a seismic event. The
29 modulation function is suitably chosen to describe earthquakes characterized by different durations.
30 The stochastic process peak theory allows to calculate damping reduction factor after the definition
31 of the probabilistic response of a simple linear visco-elastic oscillator. The variability with seismic

32 duration for different soil conditions and damping ratios is investigated. The study points out that
33 damping reduction factor is more sensitive to seismic duration in the range of high period and on
34 rigid soil with respect to other conditions. The results show that, if damping ratio or effective duration
35 values are increased, the damping reduction factor value diminishes.

36

37 **Keywords:** Ground Motion Duration, Damping Reduction Factor, Seismic response spectrum,
38 Stochastic process, random vibration theory

39

1. Introduction

Serious seismic damage observed on structures and infrastructures systems up to today [1] can be prevented by means of retrofitting interventions if the capacity of these systems and the seismic demand are properly evaluated [2]-[6]. In structural seismic design, Damping Reduction Factor (DRF) represents an effective tool for design purposes to estimate the demand by response spectra characterized also by damping ratios different from 5% as in case of structures equipped with passive energy dissipation or isolation systems. DMF modifies the values of the conventional elastic spectral response with damping ratio equal to 5% to the values corresponding to a different damping level. It is defined as the ratio between the spectral ordinate at 5% of conventional damping and the spectral ordinate at a different level of damping.

DRF finds many applications to study the behavior of structures [7], especially for the ones equipped with passive energy dissipation or isolation systems [8]-[12]. In these situations, the DRF permits to estimate the variation of the structural response (displacements and forces) due to the high supplemental damping values [13]-[16]. In addition, for inelastic structures, DRF allows to calculate the maximum displacement demand from the one of an equivalent linear system [8]. For these and other reasons the DRF is particularly suitable for the seismic design of a structure since it provides a practical evaluation of the reduction of earthquake loads for effects of structural, non-structural and supplementary energy dissipation systems. For that reason, it is selected as a key parameter in the present study.

In past years, several studies for the formulation of the DRF have been carried out by many researchers, the outcomes of which have been adopted by the main seismic codes. Different expressions for the DRF can be found in literature. Up to today, the main research efforts have been oriented to the study of the response of a simple (elastic) SDOF system with viscous damping under seismic action [17]-[23]. As a consequence, the codes introduce a DRF that depends on the damping ratio only, whereas different authors [21]-[23] showed that various parameters may affect the DRF. There are two ways to classify the parameters that much influence the DRF: by non-structural

66 parameters such as earthquake magnitude, ground motion duration (GMD), site conditions, epicentral
67 distance, etc. or by structural parameters such as damping of the structure, natural vibration period,
68 dissipation device properties (energy dissipation capacity), etc.. A very interesting topic is represented
69 by the dependence of DRF on seismological parameters. This dependence is much evident
70 considering local site conditions, source distance and magnitude of the earthquake [21]-[24]. In [25]
71 a simulation procedure to estimate the DRF based on an artificial neural network has been developed.
72 The effect of magnitude on the DRF is greater in case of large earthquakes as it was pointed out in
73 different studies [22] for structures with natural periods greater than 0.5 sec. Attention should be
74 placed in case of structures with shorter natural periods (< 0.5 sec) for which the magnitude can have
75 also contrary effects [23]. Concerning the influence of seismological parameters on DRF, Bommer
76 et al. [22] focused their studies on the GMD. The authors observed that it is possible to take into
77 account the influence of magnitude and distance by studying the effect of the GMD and the number
78 of cycles. Based on this observation, Stafford et al. [26] introduced significant equations that give the
79 DRF for different damping ratios starting from the number of cycles and the GMD. In its research,
80 Stafford concluded that a prediction model based on the GMD parameter could be used with
81 difficulties as this parameter usually is not one of the parameters elaborated and directly available in
82 earthquakes database. However, non - distinction between soil types is given by Stafford et al. [26].
83 Rosenblueth [27] suggested an equation to predict the influence of GMD on DRF and, in accordance
84 with Stafford et al. [26], concluded that the influence of GMD appears negligible for earthquake
85 GMD larger than about 20 sec.

86 The GMD finds a different definition in the models proposed by Stafford et al. [26] and Rosenblueth
87 [27] but a very good match is observed for damping ratio equal to 10%. Some discrepancies are
88 noticeable among the two models when damping ratio increases. The influence of GMD on DRF has
89 been also investigated by Anbazhagan et al. [28]. The authors choose the pseudo-spectral acceleration
90 to define the DRF and investigate how the DRF varies as a function of magnitude and GMD, distance
91 of earthquake hypocenter, classification of site (soil type), period and damping. The dependence of
92 DRF on the GMD was also analyzed by Daneshvar et al. [29] which concluded that DRF mainly

93 depends on the GMD and the frequency content that are different for each record. Zhou et al. [30]
94 studied how the DRF is affected by the effective GMD. The authors point out that greater values of
95 the damping ratio or of the effective GMD produce smaller values of DRF. However, the GMD is
96 function of distance and magnitude of ground motion and of soil type, that are parameters much more
97 common and available in ground motion database. For that reason, it is usually preferable to define a
98 function between these parameters and the DRF that indicates also a relation between DRF and GMD.
99 However, in this study the authors do not include the type of soil in the evaluation of dependence of
100 DRF with GMD.

101 Rezaeian et al. [31] propose a model to relate the DRF to the magnitude and distance to include in
102 the model the high influence of GMD. The influence of different parameters on DRF is not the same
103 in the cited studies because the sites are classified in different way and the selection of ground motions
104 is performed by different criteria. So a stochastic process is adopted in the proposed study to
105 overcome this difficulties.

106 In a previous study [32] the authors, by means of the random theory approach, investigated the effect
107 of soil type on DRF and demonstrated that not only the predominant frequency of the seismic event
108 but also the bandwidth of seismic signal affect the DRF. Since the study of the joint effect on DRF
109 of parameters such as soil type and GMD has not performed in other studies, the authors will develop
110 random vibration theory to analyse in a combined way the influence of earthquake duration and soil
111 type on DRF. GMD is a key parameter in seismic design. Since the 1950s, the peak acceleration,
112 frequency content and GMD are considered important parameters to design the structures but up to
113 today the peak acceleration and frequency content are the only parameters used in design methods.
114 The influence of GMD on DRF is investigated in the present study by means of the random vibration
115 theory: a modulated filtered stochastic process is applied on a linear single degree of freedom (SDF)
116 system and the peak theory of stochastic process is used to calculate the seismic spectrum in stochastic
117 terms. The product of a time modulation function [33] [34] and a stationary filtered stochastic process
118 gives a modulated non-stationary stochastic process. A series of two linear oscillators forced by a
119 modulated white noise process permit to obtain the linear fourth order filter that is adopted in the
120 procedure. A formulation correlating the modulating function and the GMD through the Arias

121 intensity [42] is introduced to analyze the effects of the GMD on DRF. In this way, the stochastic
122 dynamic response can be evaluated for different GMDs, properly defining the modulation function
123 and therefore a sensitivity analysis on DRF can be carried out to evaluate how DRF changes as a
124 function of different parameters. The proposed approach overcomes the limitations of the strategies
125 based on seismic records of real events, because in these it is difficult to accurately identify the
126 influence of different factors. This is pointed out by discrepancies between the various studies existing
127 in the literature.

128 The main advantage of using a stochastic approach is, on the contrary, the possibility to represent
129 seismic motion by a simple model defined by few parameters, but able to describe the most
130 seismological characteristics of real earthquakes as content of energy, frequency and GMD. On the
131 other hand, the proposed approach would require an assessment of the spectrum parameters
132 themselves on the basis of seismic models that are more consistent with the seismic scenario.

133 The study is presented in the following sections: the stochastic model of the seismic acceleration is
134 explained in section 2. The relation between the modulation function parameters and GMD is defined
135 in section 3. The evaluation of DRF in stochastic terms is developed in section 4. The results of the
136 sensitivity analysis developed considering different GMDs and soil conditions are shown and then
137 discussed in section 5. A formulation for DRF evaluation useful for practical applications is proposed
138 and compared with other existing formulations in section 6. Finally, the conclusions are given in
139 section 7.

140 **2. Stochastic Modelling of Seismic Motion**

141 Seismic acceleration is assumed as a uniformly modulated non-stationary stochastic process that is
142 calculated by the product of a time modulation function $\varphi(t)$ and a stationary process [35]. The
143 stationary part of the process is described by the well known filtered process proposed by Clough et
144 al. [36]: two linear oscillators in series, subjected to a modulated white noise process give a linear
145 fourth order filter. Ground acceleration \ddot{X}_g is given by:

$$\begin{cases}
\ddot{X}_g(t) = -\omega_p^2 X_p(t) - 2\xi_p \omega_p \dot{X}_p(t) + \omega_f^2 X_f + 2\xi_f \omega_f \dot{X}_f(t) \\
\ddot{X}_p(t) + \omega_p^2 X_p(t) + 2\xi_p \omega_p \dot{X}_p(t) = \omega_f^2 X_f + 2\xi_f \omega_f \dot{X}_f(t) \\
\ddot{X}_f(t) + 2\xi_f \omega_f \dot{X}_f(t) + \omega_f^2 X_f = -\phi(t)W(t)
\end{cases} \quad (1)$$

147 where $W(t)$ is the white noise stochastic process, with Power Spectral Density function S_0 ; $X_f(t)$ is
148 the first filter response, with frequency ω_f and damping ratio ξ_f , $X_p(t)$ is the second filter response
149 with frequency ω_p and damping ratio ξ_p ; $\phi(t)$ is the modulation function. The present research
150 assumes the Jennings' modulation function [37], below reported:

$$\phi(t) = \alpha t e^{-\beta t} \quad \alpha, \beta > 0 \quad (2)$$

152 α , β being the parameters that describe the shape of the modulation function that will be selected in
153 section 3.

154 3. Definition of modulation function considering the earthquake duration

155 Until now, GMD has been defined in different ways in literature [38] but the bracketed duration, the
156 uniform duration and the significant duration are the most used. For a given curve that shows the
157 values of the acceleration as a function of the time, the duration of the ground motion is a time
158 interval. In the case of bracketed duration, a threshold value of acceleration (usually 0.05 g) is defined.
159 The bracketed duration [39] is the time interval between the time corresponding to the first and the
160 time corresponding to the last overrun of the defined threshold value of acceleration. The choice of
161 the threshold value is different in literature and therefore this definition of GMD results subjective (it
162 can be absolute or relative e.g. 10% of Peak Ground Acceleration (PGA)). The uniform duration [40],
163 [41] is calculated as the sum of time intervals. During each time interval the acceleration values
164 overrun the threshold value of the acceleration. This definition of GMD is explained in a way similar
165 to the bracketed duration except for the interval between the thresholds. The disadvantages in the use
166 of this GMD definition are: the dependence of the GDM on the chosen threshold acceleration value;
167 the influence of small earthquakes recorded before or after the main earthquake record that could be
168 included in the GMD evaluation. The effective duration is a preferable definition of GMD because it

169 is the time interval necessary to release a given seismic energy content. The Arias intensity I_a [42]
 170 that considers the integral square of the ground acceleration, a measure of the energy content, is
 171 usually chosen to define this GDM. The Arias intensity is defined as:

$$172 \quad I_a = \frac{\pi}{2g} \int_0^{T_t} \ddot{x}_g^2(t) dt \quad (3)$$

173 where $\ddot{x}_g(t)$ is the time history of the ground acceleration, g is the acceleration of gravity and T_t is
 174 the GMD of the record. The time intervals T_{5-75} and T_{5-95} between 5%-75% and 5%-95% of the Arias
 175 intensity (I_a) are respectively the two measures of significant duration most used in literature.

176 In this study, in order to analyze the influence of GMD on DRF, T_{5-95} is considered, as it is one of the
 177 most common measure of GMD and it can be related to magnitude, distance and soil type. Different
 178 empirical formulation have been proposed in literature for effective duration [43]-[46] which consider
 179 the dependence on magnitude, distance and soil condition. The outcome was that effective duration
 180 increases with distance, magnitude and moving from rock to soft soil. Among these three influencing
 181 parameters, soil type has a larger influence than distance.

182 The present research deals with the evaluation of the influence of the effective duration on DRF for
 183 different soil conditions. To develop a suitable model for this analysis, a formulation correlating the
 184 modulating function and T_{5-95} (effective duration) throughout the mean value of I_a is obtained. In this
 185 way, stochastic dynamic response can be evaluated for different GMDs, properly defining the
 186 modulation function. In order to achieve the correlation between GMD and modulation function, the
 187 two parameters α and β in Eq. 2 are obtained by an identification procedure. Introducing the time
 188 t_m where the modulation function exhibits its maximum value, parameters α and β are expressed
 189 as functions of this unknown parameter from the simultaneous equations:

$$190 \quad \begin{cases} \phi(t_m) = 1 \\ \frac{d}{dt} \phi(t_m) = 0 \end{cases} \quad (4)$$

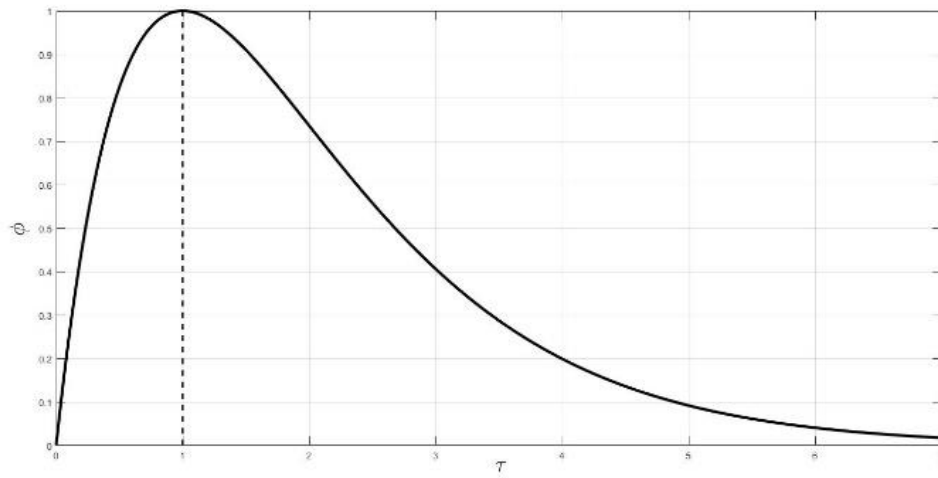
191 The two parameters α and β are then evaluated as function of t_m :

192
$$\beta = \frac{1}{t_m} \quad (5)$$

193
$$\alpha = \frac{e}{t_m} \quad (6)$$

194 The dimensionless time ratio $\tau = \frac{T_t}{t_m}$ can be introduced in Eq. (2), so obtaining:

195
$$\phi(\tau) = \tau e^{(1-\tau)} \quad (7)$$



196
197 *Figure 1: Modulation function (Φ) in dimensionless time (τ)*

198 The time values at which 5 % and 95 % of the Arias intensity is reached can be used to evaluate the
199 effective duration T_{5-95} . In stochastic terms, the mean value of I_a could be evaluated as:

200
$$\mu[I_a] = \frac{\pi}{2g} \int_0^{T_t} \langle \ddot{x}_g^2(t) \rangle dt = \frac{\pi}{2g} \sigma_{\ddot{x}_g}^2 \psi_a(T_t) \quad (8)$$

201 where T_t is the total duration of the acceleration record, $\sigma_{\ddot{x}_g}^2$ is the variance calculated for the
202 acceleration of the ground, $\langle \ddot{x}_g^2(t) \rangle$ denotes the expected value of the square of \ddot{x}_g and $\psi_a(T_t)$ is
203 defined by:

204
$$\psi_a(T_t) = \int_0^{T_t} \phi^2(t) dt \quad (9)$$

205 Now using Eq. (7), Eq. (9) becomes:

206
$$\int_0^{\rho} \phi(\tau)^2 d\tau = \frac{1}{4} e^2 (1 - e^{-2\rho} (1 + 2\rho(1 + \rho))) \quad (10)$$

207 where $\rho = \frac{T}{t_m}$. At the end of the phenomenon ($T = \infty$), it results:

208
$$\psi_a(\infty) = \int_0^{\infty} \phi(\tau)^2 d\tau = \frac{e^2}{4} \quad (11)$$

209 So the dimensionless time ρ_k necessary to release the k% of the total I_a is the solution of the following
210 equation:

211
$$\int_0^{\rho_k} \phi(\tau)^2 d\tau = k \int_0^{\infty} \phi(\tau)^2 d\tau \quad (12)$$

212 that means in implicit form:

213
$$\frac{1}{4} e^2 (1 - k - e^{-2\rho_k} (1 + 2\rho_k (1 + \rho_k))) = 0 \quad (13)$$

214 Equation (12) allows the definition of the ρ_5 and ρ_{95} values corresponding to the 5% and the 95% of
215 the energy I_a calculated on the modulation function respectively. The values so obtained are:

216
$$\begin{aligned} \rho_5 &= 0.40884 \\ \rho_{95} &= 3.1478 \end{aligned} \quad (14)$$

217 Thus the values t_m corresponding to the selected effective duration T_{5-95} can be determined by the
218 definition of the ratio ρ :

219
$$\begin{aligned} T_5 &= 0.40884 t_m \\ T_{95} &= 3.1478 t_m \end{aligned} \quad (15)$$

220 Finally, the effective duration is $T_{5-95} = 2.7390 t_m$, so that it is possible to define t_m as:

221
$$t_m = \frac{T_{5-95}}{2.7390} \quad (16)$$

222

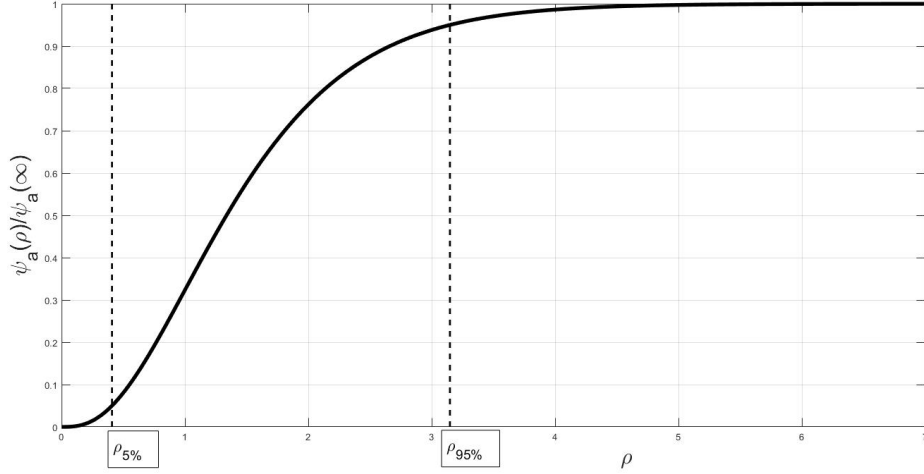


Figure 2: $\psi_a(\rho)/\psi_a(\infty)$ in dimensionless time scale (ρ)

223
224

4. Evaluation of Damping Reduction Factor by peak theory

225

226 In this section, the seismic ground acceleration action $\ddot{X}_g(t)$ given by Eq. (1) is applied on a simple
227 linear-viscous SDOF system to evaluate the DRF in stochastic meaning. For this system, the motion
228 equation is:

$$\ddot{X}_s(t) + 2\xi\omega\dot{X}_s(t) + \omega^2 X_s(t) = -\ddot{X}_g(t) \quad (17)$$

230 where X_s is system-ground relative displacement, ω is the natural frequency and ξ is the damping
231 ratio:

$$\omega = \sqrt{\frac{k}{m}} \text{ and } \xi = \frac{c}{2\sqrt{km}}, \quad (18)$$

233 k and m being the system mass and stiffness, respectively.

234 In the state-space, the motion equation of the system becomes:

$$\dot{\mathbf{Z}}(t) = \mathbf{A}\mathbf{Z}(t) + \mathbf{F}(t). \quad (19)$$

236 where \mathbf{F} is the force vector and \mathbf{Z} is the state-space vector:

$$\mathbf{Z} = (X_s, X_p, X_f, \dot{X}_s, \dot{X}_p, \dot{X}_f)^T \quad (20)$$

$$\mathbf{F} = (0, 0, 0, 0, 0, -\varphi(t)w(t))^T \quad (21)$$

239 Finally \mathbf{A} is the state matrix:

$$240 \quad \mathbf{A} = \begin{pmatrix} 0 & 0 & 0 & 1 & 0 & 0 \\ 0 & 0 & 0 & 0 & 1 & 0 \\ 0 & 0 & 0 & 0 & 0 & 1 \\ -\omega^2 & \omega_p^2 & -\omega_f^2 & -2\xi\omega & +2\omega_p\xi_p & -2\omega_f\xi_f \\ 0 & -\omega_p^2 & +\omega_f^2 & 0 & -2\omega_p\xi_p & +2\omega_f\xi_f \\ 0 & 0 & -\omega_f^2 & 0 & 0 & -2\omega_f\xi_f \end{pmatrix} \quad (22)$$

241 The matrix Lyapunov differential equation [47]-[54] can be used to calculate the stochastic response
 242 of the system when it is excited by the non-stationary modulated Clough and Penzien stochastic
 243 process:

$$244 \quad \dot{\mathbf{R}}(t) = \mathbf{A}\mathbf{R}(t) + \mathbf{R}(t)\mathbf{A}^T + \mathbf{B}(t) \quad (23)$$

245 where $\mathbf{R}(t) = \langle \mathbf{Z}\mathbf{Z}^T \rangle$ is the covariance matrix and $\mathbf{B}(t)$ is a matrix that is square and has all elements
 246 equal to zero except for the last one that assumes the value $2\pi S_0\phi(t)^2$.

247 For the analyzed system, a definition of the displacement spectrum is:

$$248 \quad S_d = |X_s(t)|_{max} \quad (24)$$

249 The DRF (η) parameter permits to approximate the high damped elastic response spectrum (S_d)
 250 starting from the 5% damped one ($S_{d,\xi=5\%}$):

$$251 \quad S_d = \eta S_{d,\xi=5\%} \quad (25)$$

252 where ζ is the damping ratio that is greater than 5% for the high damped system.

253 A seismic response spectrum gives the maximum displacement or acceleration response of a
 254 SDOF system when a recorded earthquake [4], [6], 5[55][61] is applied as a function of the natural
 255 period of the system. Different relations are obtained for different values of structural damping. From
 256 a stochastic point of view, the response spectrum is still a relation between the maximum acceleration
 257 or displacement response of a SDOF system, that is subjected to a ground motion, and the natural
 258 period of the SDOF system but the maximum response and the ground motion are considered in
 259 stochastic terms. Different values of structural damping again give different response spectra.

260 In the present paper the authors propose a procedure to calculate the DRF value starting from the
 261 definition of the stochastic displacement spectrum by mean of the peak theory. This theory assumes
 262 that the maximum response of a SDOF system in displacement X_s^{\max} is the displacement value that
 263 is not overrun with a fixed value of the probability P_f^* . For this reason the analysis focuses on the
 264 evaluation of this maximum displacement that, from a mathematical formulation, is the displacement
 265 threshold b that will not be exceeded with a probability P_f^* during the system lifetime [62]. If this
 266 problem is analyzed for a generic process X and for a threshold b , the Vanmarcke formula [63] gives
 267 the probability that the process X exceeds the threshold b :

$$268 \quad P(t, b) = 1 - \exp\left(-\int_0^t \alpha(\tau) d\tau\right) \quad (26)$$

269 where the expected decay rate $\alpha(\tau)$ is:

$$270 \quad \alpha(\tau) = v_X(b, t) \frac{1 - \exp\left[-\frac{v_R^+(b, t)}{v_X(b, t)}\right]}{1 - \frac{v_X^+(b, t)}{v_X^+(0, t)}} \quad (27)$$

271 $v_X(b, t) = v_X^+(b, t) + v_X^-(b, t)$ being the expected rate of the response that exceeds the threshold. The
 272 up and down crossing expected rates are given by [64]:

$$273 \quad v_X^+(b, t) = \int_b^{\infty} (\dot{x} - \dot{b}) f_{X\dot{X}}(t, b; t, \dot{x}) d\dot{x} \quad (28)$$

$$v_X^-(b, t) = \int_{-\infty}^b (\dot{b} - \dot{x}) f_{X\dot{X}}(t, -b; t, \dot{x}) d\dot{x}$$

274 where $f_{X\dot{X}}(t, b; t, \dot{x})$ is the joint probability density function (JPDF) of X and \dot{X} .

275 In Eq. (14) the expected up-crossing rate of the envelope process $R(t)$ is indicated with $v_R^+(b, t)$ and
 276 $R(t)$ can be expressed as:

$$277 \quad R(t) = \sqrt{X(t) + \hat{X}^2(t)} \quad (29)$$

278 where $\hat{X}(t)$ is the Hilbert transform of $X(t)$.

279 In Eq. (27) $v_r^+(b, t)$ is obtained from Eq. (15) replacing \dot{x} and $f_{x\dot{x}}(t, b; t, \dot{x})$ with \dot{r} and $f_{r\dot{r}}(t, r; t, \dot{r})$
 280 respectively if the JPDF $f_{r\dot{r}}(t, r; t, \dot{r})$ is available.

281 For convenience, the above crossing rates are evaluated in a normalized way by introducing the
 282 normalized variables:

$$283 \quad Y(t) = \frac{X(t)}{\sigma_x(t)} \quad (30)$$

$$284 \quad Q(t) = \sqrt{Y(t) + \hat{Y}^2(t)} = \frac{R(t)}{\sigma_x(t)} \quad \kappa(t) = \frac{b}{\sigma_x(t)} \quad (31)$$

285 $\sigma_x(t)$ being the standard deviation of X process and $\hat{Y}(t)$ the Hilbert transform of $Y(t)$.

286 Since $\hat{Y}(t)$ and $Y(t)$ result uncorrelated, Eqs. (15) become:

$$287 \quad v_x^+(t, b) = v_y^+(t, \kappa) = \omega_0 \phi(\kappa) \left[\phi\left(\frac{\dot{\kappa}}{\omega_0}\right) - \frac{\dot{\kappa}}{\omega_0} \Phi\left(-\frac{\dot{\kappa}}{\omega_0}\right) \right] \quad (32)$$

$$288 \quad v_x^-(t, b) = v_y^-(t, \kappa) = \omega_0 \phi(\kappa) \left[\phi\left(\frac{\dot{\kappa}}{\omega_0}\right) + \frac{\dot{\kappa}}{\omega_0} \Phi\left(-\frac{\dot{\kappa}}{\omega_0}\right) \right] \quad (33)$$

289 where ϕ is the standard normal density function, Φ is the standard normal distribution function and

290 ω_0 is the standard deviation of $\dot{Y}(t)$, given by:

$$291 \quad \omega_0^2 = E[\dot{Y}^2(t)] = E\left[\frac{\sigma_x(t)\dot{X}(t) - X(t)\dot{\sigma}_x(t)}{\sigma_x^2(t)}\right] \quad (34)$$

$$= \frac{\sigma_{\dot{X}}(t)}{\sigma_x^2(t)} - 2\frac{\dot{\sigma}_x(t)}{\sigma_x^3(t)}c_{x\dot{x}}(t) + \frac{\dot{\sigma}_x^2(t)}{\sigma_x^2(t)}$$

292 The functions $Q(t)$ and $\dot{Q}(t)$ are mutually independent in the case of a normal process, with the

293 Rayleigh and normal distribution respectively given by:

$$294 \quad f_Q(q) = q \exp\left(-\frac{q^2}{2}\right) \quad (35)$$

$$295 \quad f_{\dot{Q}}(\dot{q}) = \frac{2}{\sqrt{2\pi(\omega_0^2 - \lambda^2)}} \exp\left(-\frac{1}{2} \frac{\dot{q}^2}{(\omega_0^2 - \lambda^2)}\right) \quad (36)$$

296 where $\lambda(t)$ is the covariance of $Y(t)$ and $\dot{Y}(t)$. Since $X(t)$ and $\hat{X}(t)$ are uncorrelated, $\hat{X}(t)$ and $\dot{\hat{X}}(t)$
 297 are uncorrelated too. Starting from the above equations, it is simple to introduce the relation:

$$298 \quad \lambda(t) = E\left[Y(t)\dot{Y}(t)\right] = E\left[\frac{X(t)}{\sigma_X(t)} \frac{\sigma_X(t)\dot{\hat{X}}(t) - \hat{X}(t)\dot{\sigma}_X(t)}{\sigma_X^2(t)}\right] = \frac{c_{X\dot{X}}(t)}{\sigma_X^2(t)} \quad (37)$$

299 Then the evaluation of the up-crossing rate for the envelope is possible by:

$$300 \quad \nu_R^+(t, b) = \nu_Q^+(t, \kappa) = f_Q(\kappa) \int_{\dot{\eta}}^{\infty} (s - \dot{\kappa}) f_{\dot{Q}}(s) ds = \quad (38)$$

$$\sqrt{\omega_0^2 - \lambda^2} \kappa e^{-\frac{\kappa^2}{2}} \left[\phi\left(\frac{\dot{\kappa}}{\sqrt{\omega_0^2 - \lambda^2}}\right) - \frac{\dot{\kappa}}{\sqrt{\omega_0^2 - \lambda^2}} \Phi\left(-\frac{\dot{\kappa}}{\sqrt{\omega_0^2 - \lambda^2}}\right) \right]$$

301 If $\sigma_X^2(t)$, $\sigma_{\dot{X}}^2(t)$, $c_{X\dot{X}}(t)$ and $c_{\dot{X}\dot{X}}(t)$ are available, then the crossing rates of $X(t)$ and $R(t)$ can be
 302 evaluated directly. The variation of the natural period of the SDOF allows to calculate the
 303 displacement spectrum. $X_{\max}^{P^*}(t)$ is the maximum displacement such that the probability that $X(t)$ will
 304 exceed the domain $[-X_{\max}^P, +X_{\max}^P]$ is equal to a given value P^* . This inverse problem can be solved
 305 by a numerical approach as described in [62].

306 5. Analysis results

307 In this section, a sensitivity analysis on DRF is carried out considering the effect of natural period,
 308 damping ratio, soil type and effective duration. More in details, different effective durations are
 309 considered, and modulation function parameters are identified by the procedure described in section
 310 4. A wide range of GMD is considered, in order to cover all possible earthquakes. Different soil
 311 conditions are analyzed (soft, medium and rigid) by assigning the Clough and Penzien model
 312 parameters as reported in Table 1. In the analysis it is assumed $P^* = 10^{-3}$.

313
 314
 315
 316

Soil type	ω_p (rad/sec)	ξ_p	ω_c (rad/sec)	ξ_c
Rigid	15	0.6	1.5	0.6
Medium	10	0.4	1	0.6
Soft	5	0.2	0.5	0.6

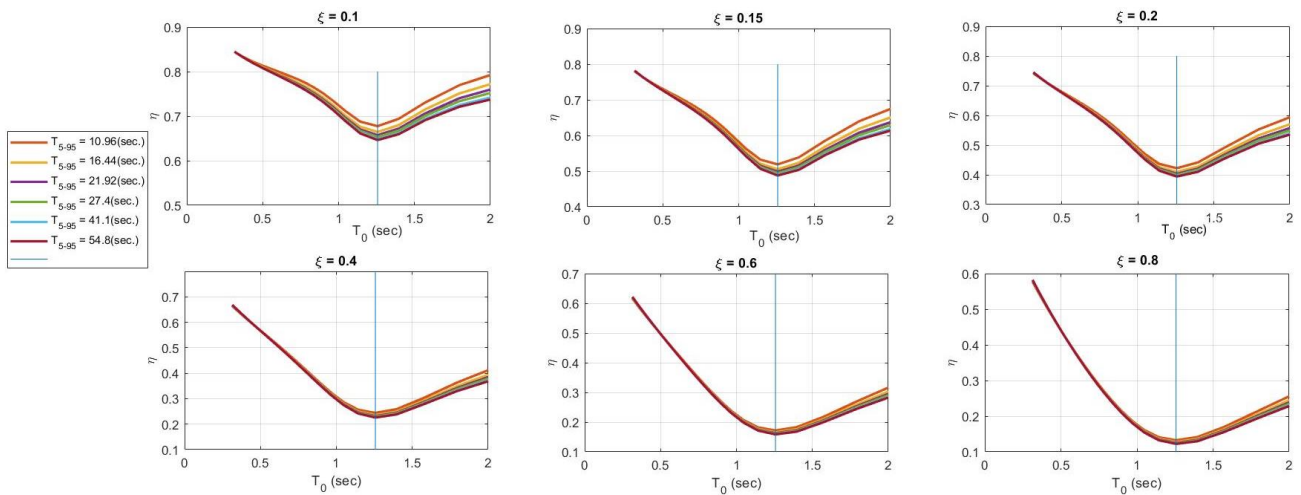
Table 1 Filter parameters for different soil types

317
318
319

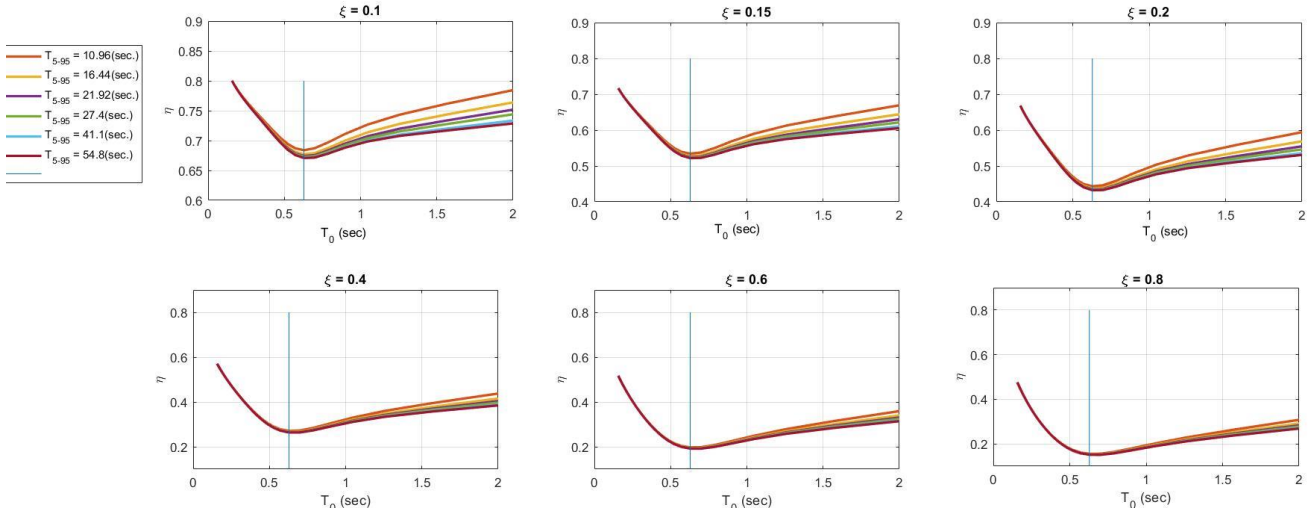
320 Figures 3 - 5 show the variability of DRF (η) for different soil conditions versus the system natural
321 period $T_0 = 2\pi / \omega$. Each plot corresponds to an assigned value of the system damping ratio ξ . Six
322 values of ξ are considered: 0.10, 0.15, 0.20, 0.40, 0.60 and 0.80. Vertical line defines the ground
323 motion predominant period $T_f = 2\pi / \omega_f$. Figure 3 shows the results for a soft soil. Different colored
324 lines correspond to different values of the effective duration T_{5-95} , which varies in the range 10.94s -
325 54.80s. The dependences between the parameters damping ratio, structural vibration period, soil type
326 and GMD are represented by means of the plots in Figures 3 - 5. The DRF shows a period-dependent
327 nature in Figure 3. It is worth noting that all curves show the same variability as T_0 varies and moves
328 downwards and as the damping ratio increases in the considered range. The lowest values of DRF
329 occurs when the natural period T_0 equals the predominant period of earthquake T_f . In detail, for T_0
330 $< T_f$ the DRF decreases with the increase of T_0 and reaches a minimum in T_f . Then, for $T_0 > T_f$ the
331 DRF increases with the increase of the natural period T_0 . The DRF tends to assume a unity value in
332 correspondence of the lowest or highest values of period. This can be explained by the fact that the
333 forces can be independent from the damping ratio in a very stiff or very flexible structure. It also
334 emerges that DRF value decreases as damping ratio ξ increases. These results have been observed by
335 Zhou et al. [30]. In addition, when period changes the DRF variation seems lower for low damping
336 ratio. For example for $\xi = 0.1$ (Figure 3), DRF varies between 0.84 and 0.64 (for a GMD of 54.8 s),
337 whereas for $\xi = 0.8$, DRF varies between 0.57 and 0.12 (for a GMD of 54.8 s).

338 With regard to the variability of DRF with GMD, that is the main topic of this study, two different
339 considerations can be carried out: firstly, it is noticed that as the GMD increases, the DRF decreases

340 and the plots move downwards. This variability of DRF with GMD is in agreement with the studies
 341 from Bommer et al. [22] and Zhou et al. [30]. These authors observed a decrease of DRF when GMD
 342 increase. In addition, results show a larger variability of DRF with GMD in the range of high natural
 343 periods. The results of these studies make evident that the GMD has important effects on DRF and
 344 this should be considered in engineering implications. Secondly, the influence of earthquake GMD
 345 depends on damping ratio and it seems larger for the system with lower damping ratio and tends to
 346 reduce as the damping ratio increases. Later we will see that this is not always true.
 347 Figures 4 and 5 show the results of the sensitivity analysis for medium and rigid soils. Firstly, it is
 348 observed that the soil type affects the DRF and more precisely DRF is larger for soft soil. This result
 349 agrees with the ones presented by Lin et al. [20]: the soil type has a significant effect on DRF
 350 especially for very stiff and rock sites. The aspects related to the influence of soil type on DRF have
 351 been discussed in a previous study by the authors to which reference is made [32]. With regard to the
 352 variability of DRF with earthquake effective duration that is the topic of this study, the same
 353 variability of the DRF, already observed in the case of soft soil, is observed for medium and rigid
 354 soils when GMD varies.

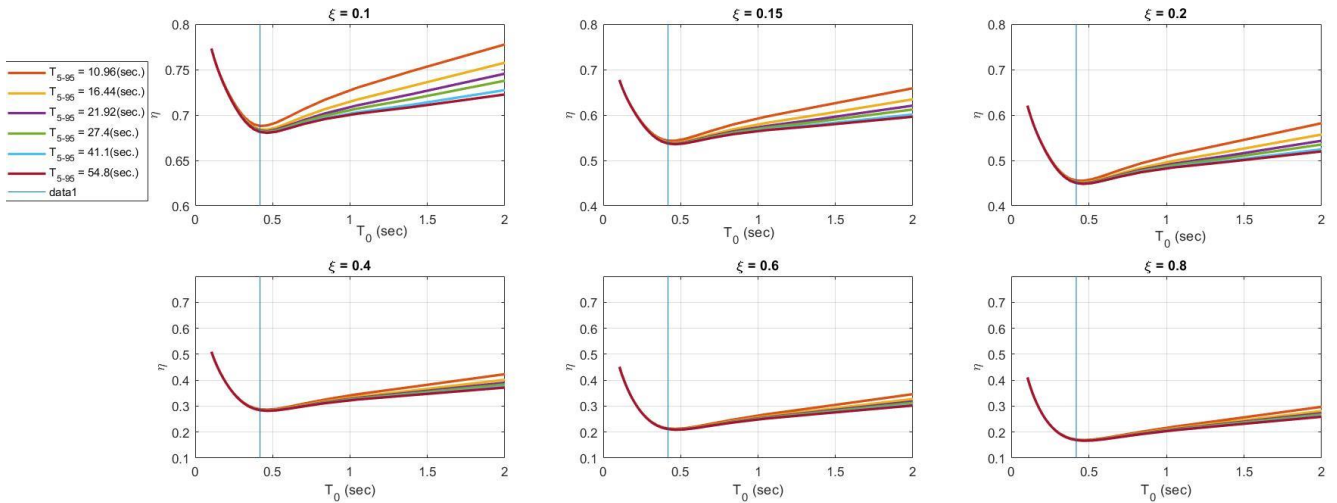


355
 356 Figure 3 Variability of DRF (η) with system natural period (T_0) for soft soil. The ground motion
 357 predominant period (T_f) is the blue line.



358
359
360

Figure 4 Variability of DRF (η) with system natural period (T_0) for medium soil. The ground motion predominant period (T_r) is the blue line.



361
362
363

Figure 5 Variability of DRF (η) with system natural period (T_0) for rigid soil. The ground motion predominant period (T_r) is the blue line.

364 Moreover, the dependency of DRF on effective duration is more evident in these two cases with
365 respect to soft soil. Also for medium and rigid soil it is observed that the variability of DRF is more
366 evident for small values of structural damping ($\xi = 0.10 - 0.20$) while tends to be negligible for
367 greater values.

368 To better analyze the influence of natural period and damping ratio on the variation of DRF as a
369 function of the effective duration, it is useful to analyze Figs. 6 - 8, representing the DRF (η) versus
370 where the effective duration (T_{5-95}). Different colored lines correspond to different values of system
371 damping ratio (ξ); the 4 sub-figures correspond to different system natural periods T_0 ($T_0=0.5$ sec,
372 $T_0=1$ sec, $T_0=1.5$ sec, $T_0=2$ sec).

373 Firstly, the case of soft soil is analyzed. It is observed that earthquake GMD does not affect the DRF
374 for system with low natural period ($T_0=0.5$ sec), except for earthquakes with a very short duration.
375 If an exception is made for the curve corresponding to the lowest value of the damping ratio $\xi =0.10$,
376 the curves are practically horizontal. When the natural periods of the system increase, a greater
377 influence of the GMD on the DRF is observed, even for high values of damping ratio. The largest
378 effects of the GMDs are for the system with natural period $T=2$ sec. In this case, the DRF varies
379 between 0.82 and 0.72 (values evaluated for $\xi =0.10$). This variability is important since it leads to
380 a 12% reduction of the spectral response and the implication in practical engineering applications are
381 relevant. As before mentioned, a greater GMD value means a greater time window in which the
382 seismic recording is analyzed. If the GMD increases, the number of cycles of the seismic event
383 increases and so also damping effects on the response of the system increase. Consequently this
384 produces [65] the decrease of DRF value. By observing in detail plots in Figs 6-8, one can observe
385 that DRF variation with GMD is significant in the initial part and then it reaches gradually a steady
386 state. Generally, it is observed that for a GMD greater than 20 sec the GMD of the excitation does
387 not affect DRF. This result agrees with Stafford et al. [66]. This outcome is also consistent with the
388 conclusions from Zhou et al [30]. The authors concluded that the maximum displacement curve shows
389 a plateau without increasing further in the case of a system on which a higher number of cycles is
390 applied. This study is based on the analysis of the harmonic excitation of SDOF and the results show
391 that DRF is almost constant for each damping value. In addition, it is observed that, at all damping
392 ratio values, the variation trends of DRF with the effective duration are consistent with each other.
393 The greatest variability of DRF is observed for $T_0=2$ sec. The same considerations can be made by
394 observing the graphs in Figs 7 and 8, which refer to a medium and rigid soil, respectively. As already
395 mentioned, for this last type of soil the greater variability of DRF with the earthquake GMD can be
396 observed.

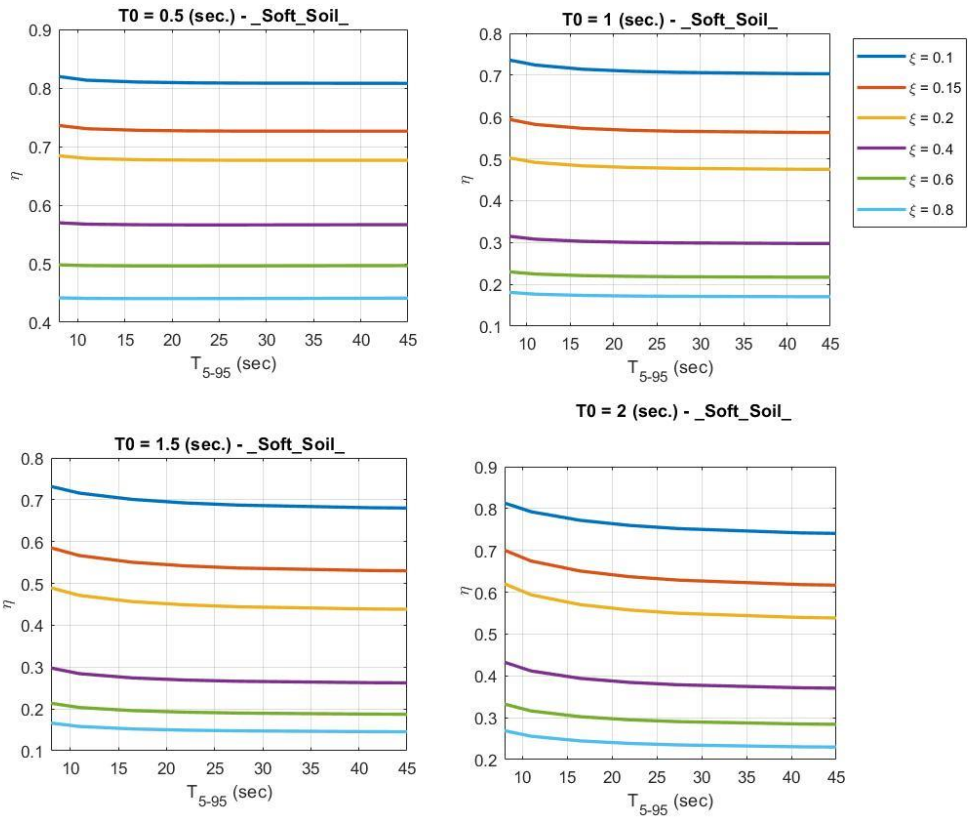


Figure 6 Variability of DRF (η) with earthquake effective duration (T_{5-95}) for soft soil; T_0 is the system natural period.

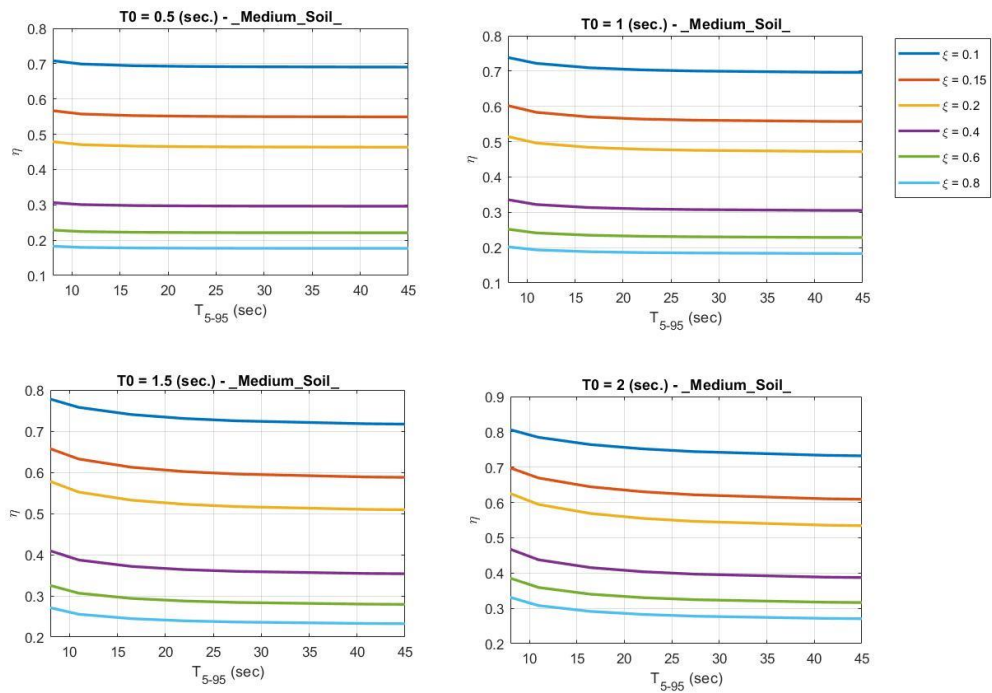


Figure 7 Variability of DRF (η) with earthquake effective duration (T_{5-95}) for medium soil; T_0 is the system natural period.

397
398
399

400
401
402
403

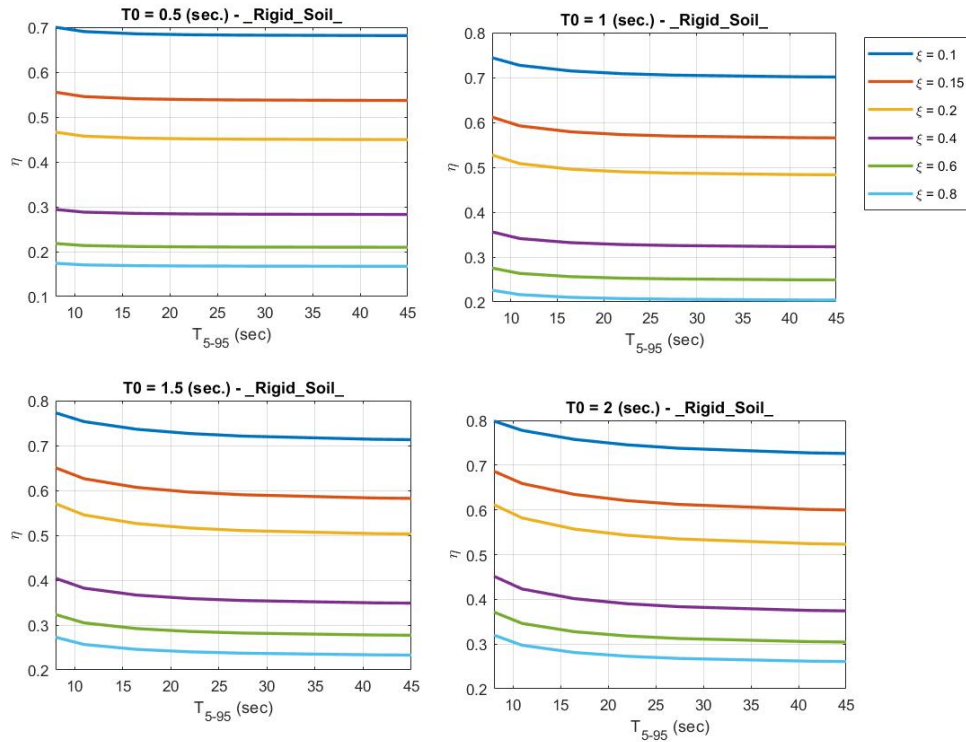


Figure 8 Variability of DRF (η) with earthquake effective duration (T_{5-95}) for rigid soil; T_0 is the system natural period.

404

405

406

407

408

409

410

411

412

413

414

415

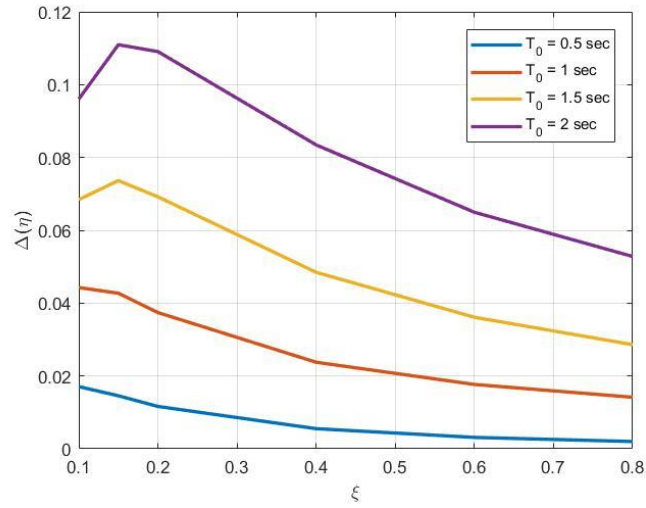
416

417

418

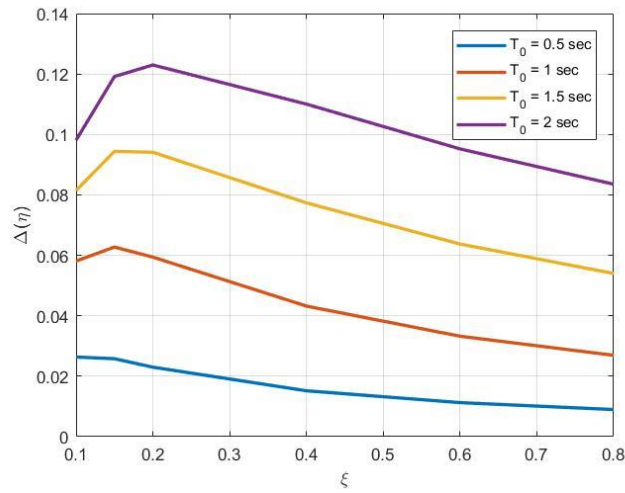
419

In order to evaluate the amount of the DRF variation with GMD and therefore the engineering implications, in Figs 9 - 11 the maximum variability of DRF ($\Delta(\eta)$), that is the DRF value evaluated for the lower effective duration minus the DRF value evaluated for the larger effective duration, is shown. All soil conditions are considered. From Fig. 9 (soft soil), it can be firstly observed that the influence of the effective duration on DRF is more relevant in the range of high periods. The maximum variation equal to 0.11 is for $T_0=2$ s and $\xi =0.15$. For $T_0=0.5$ sec the variability of DRF with effective duration always decreases as the damping ratio increases, whereas as the system becomes more deformable a different behavior can be observed. In fact, as the damping ratio increases the effect of effective duration on DRF firstly increases and then decreases as the damping ratio grows up. This tendency is more evident for the system with the largest natural period considered in this study ($T_0=2$ sec). From Figures 10 and 11 (medium and rigid soil) an analogous behavior can be observed.



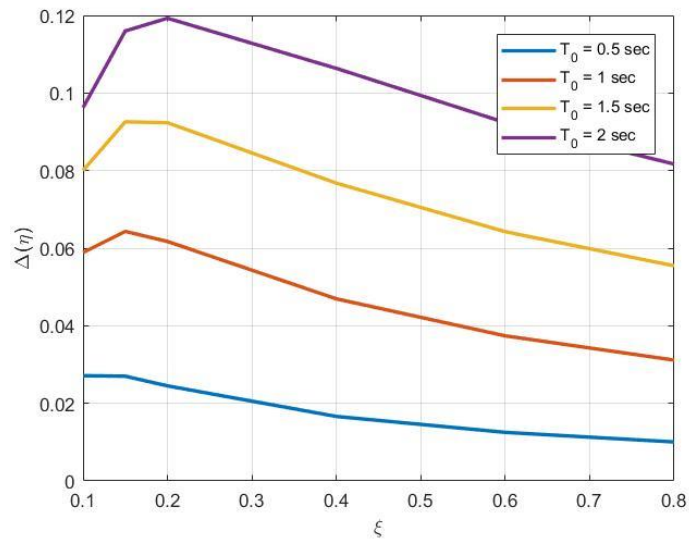
420
421

Figure 9 Maximum variability of DRF ($\Delta(\eta)$) with system damping ratio for soft soil; T_0 is the system natural period.



422
423
424

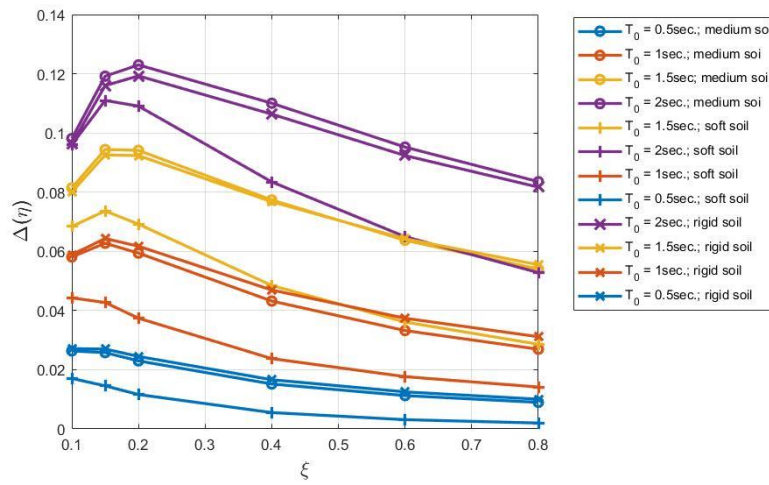
Figure 10 Maximum variability of DRF ($\Delta(\eta)$) with system damping ratio for medium soil; T_0 is the system natural period.



425
426

Figure 11 Maximum variability of DRF ($\Delta(\eta)$) with system damping ratio for rigid soil; T_0 is the system natural period.

427 Figure 12 shows the maximum DRF variability $\Delta(\eta)$ as damping ratio increases. The different colored
 428 lines correspond to the 4 structural periods analyzed, while the three symbols on the curves identify
 429 the three soil types. The variability of DRF with GMD is influenced by the natural periods of the
 430 system, by the damping ratio and by the soil type. The greater variability is for deformable systems
 431 on rigid soils and generally in the range of low damping ratio values, although a precise damping
 432 value at which the maximum variability is obtained can be identified. For rigid soil, the maximum
 433 DRF variability $\Delta(\eta)$ is 0.125 for $\xi = 0.2$.



434
 435 Figure 12 Comparison of maximum variability of DRF ($\Delta(\eta)$) with system damping ratio for different soils; T_0 is the system natural
 436 period.

437 6. Proposed DRF formulation

439 In this section a novel formulation for the DRF useful for practical application, which, in addition to
 440 the period and the damping, also accounts for the effects of GMD and soil characteristics is furnished:

$$441 \quad DRF(\xi, T_0, T_{5-95}) = \left(\frac{1 + \psi(T_0) \left(\frac{T_{5-95}}{T_0} \right) \xi}{1 + \psi(T_0) \left(\frac{T_{5-95}}{T_0} \right) 0.05} \right)^{\vartheta(T_0)} \quad (39)$$

442 where

$$443 \quad \psi(T_0) = \alpha e^{-\beta T_0} \quad (40)$$

$$444 \quad \vartheta(T_0) = \chi + \delta T_0 \quad (41)$$

445 Nonlinear multiple regressions are carried out using a Matlab code [67] to acquire the relationship
 446 that assures the best-fit of the DRF with the influence of the soil type, GMD, damping ratio and
 447 natural period. The parameters in Eqs. (40) and (41) are given in Table 2.

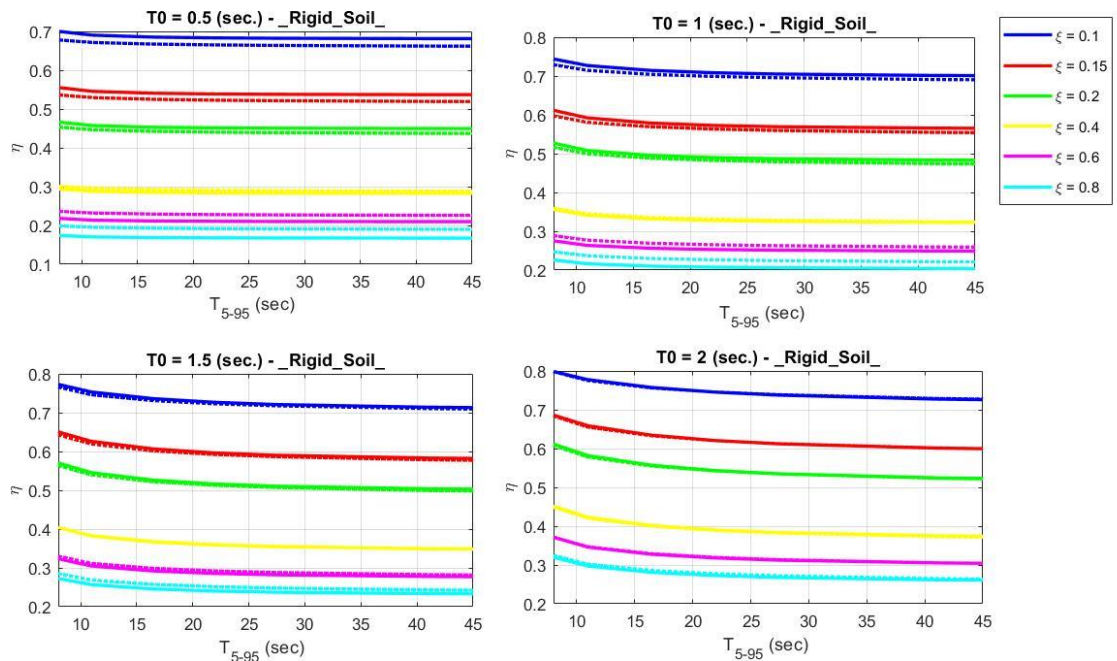
448 In order to assess the efficiency of developed regression, first a comparison with results of stochastic
 449 analysis is shown. Figures 13-15 show the comparison between the proposed formulation and the
 450 results from the stochastic analysis for different soils. The dashed line is the proposed formulation
 451 while the continuous line is the result obtained by the stochastic analysis. A very good agreement is
 452 noticeable for rigid soil and medium soil whereas for soft soil some discrepancies can be observed in
 453 the range of high natural periods. For rigid soil, except for $T_0=0.5$ sec, the curves are practically
 454 coincident each other.

455
 456

Table 2 Parameters in equations (40) and (41) for different soil types

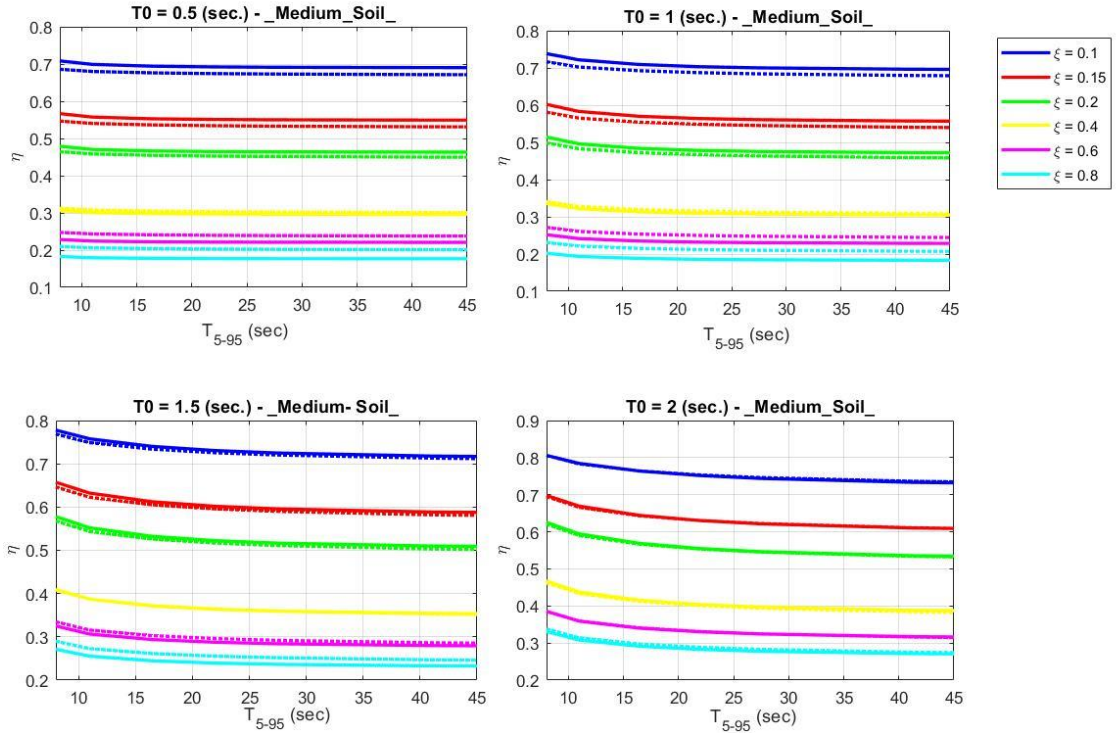
Soil type	α	β	χ	δ
Rigid	16.3450	0.4626	0.4626	-0.6286
Medium	18.9182	0.5615	0.0677	-0.6259
Soft	171.8278	2.0195	-0.1364	-0.3302

457



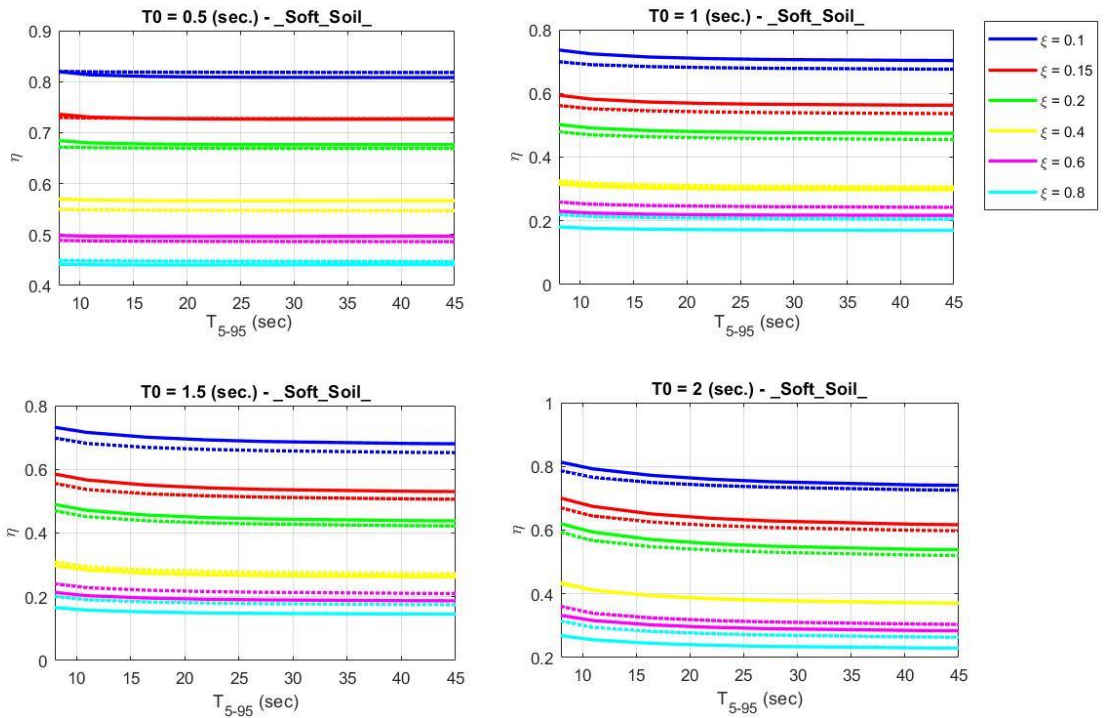
458
 459
 460

Figure 13 Comparison between the proposed formulation (Dashed line) and the results from stochastic analysis (continuous line) for DRF (η) in case of rigid soil; ξ is the damping ratio.



461
462
463

Figure 14 Comparison between the proposed formulation (Dashed line) and the results from stochastic analysis (continuous line) for DRF (η) in case of medium soil; ξ is the damping ratio.

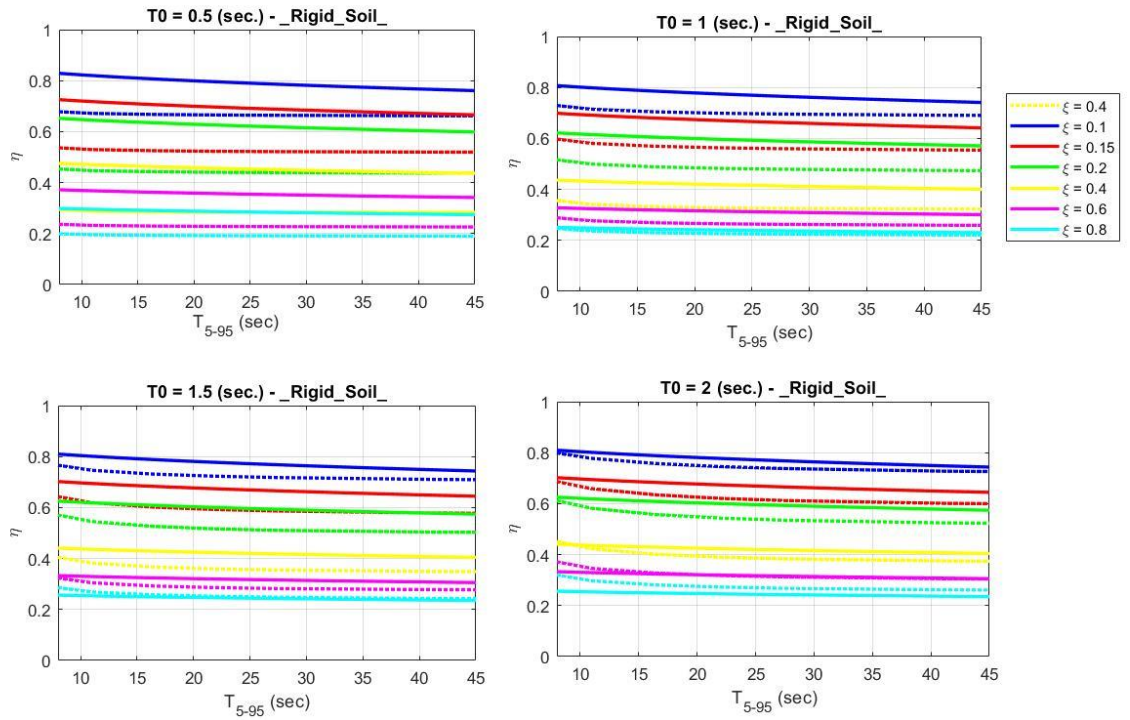


464
465
466
467

Figure 15 Comparison between proposed formulation (Dashed line) and results from stochastic analysis (continuous line) for DRF (η) in case of soft soil; ξ is the damping ratio.

468 Finally, it would be interesting to compare the proposed formulation with results performed by other
469 studies. However as explained in the introduction, there are not studies which consider simultaneously

470 the effect of soil type and GMD on DRF. Therefore, a possibility is to compare the results attained
 471 by proposed formulation with results reported in [69], in which only the influence of damping ratio,
 472 natural period and duration, but not type of soil, is considered.
 473 The results of this comparison are shown for different soils in Figures 16-18. The comparison shows
 474 that in some cases the Zhou's formula overestimates the value of the DRF compared to the proposed
 475 formulation. This is generally true for low natural periods and for low damping. The formulations
 476 proposed, on the contrary, are in good agreement for $T_0=2.0$ s and for high damping ratio.



477
 478 Figure 16 Comparison between proposed formulation (Dashed line) and results in [69] in case of rigid soil; ξ is the damping ratio.
 479

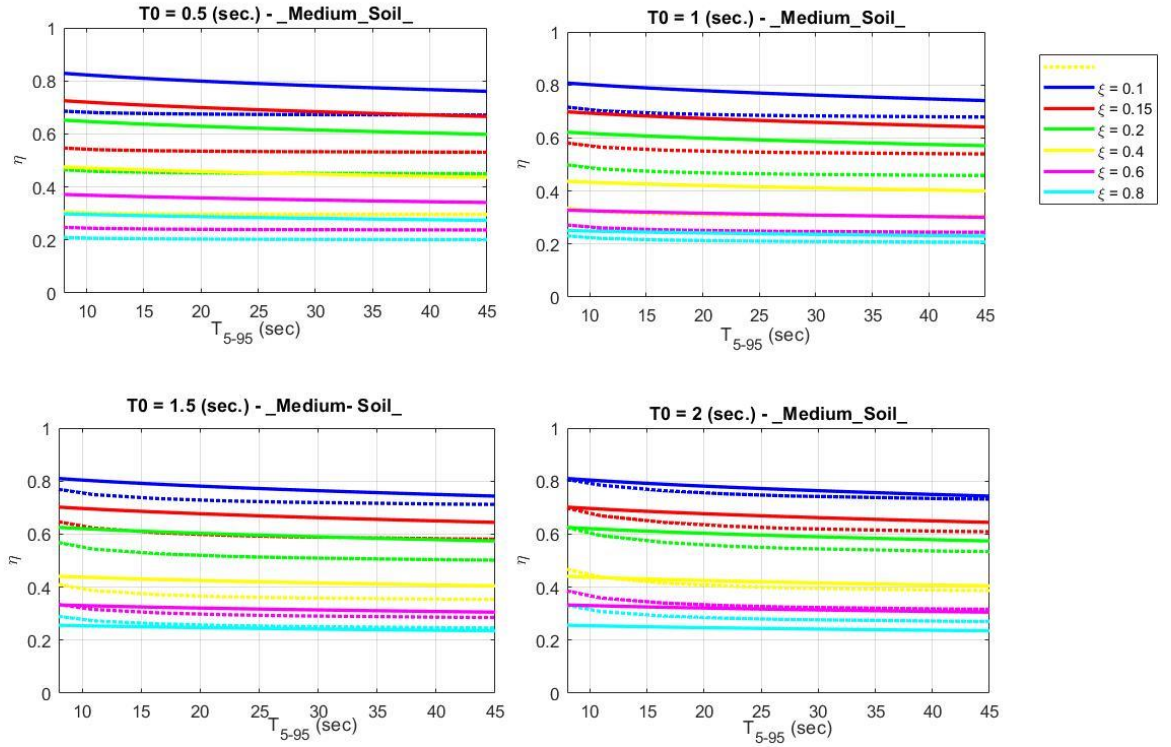


Figure 17 Comparison between proposed formulation (Dashed line) and results in [69] in case of medium soil; ξ is the damping ratio.

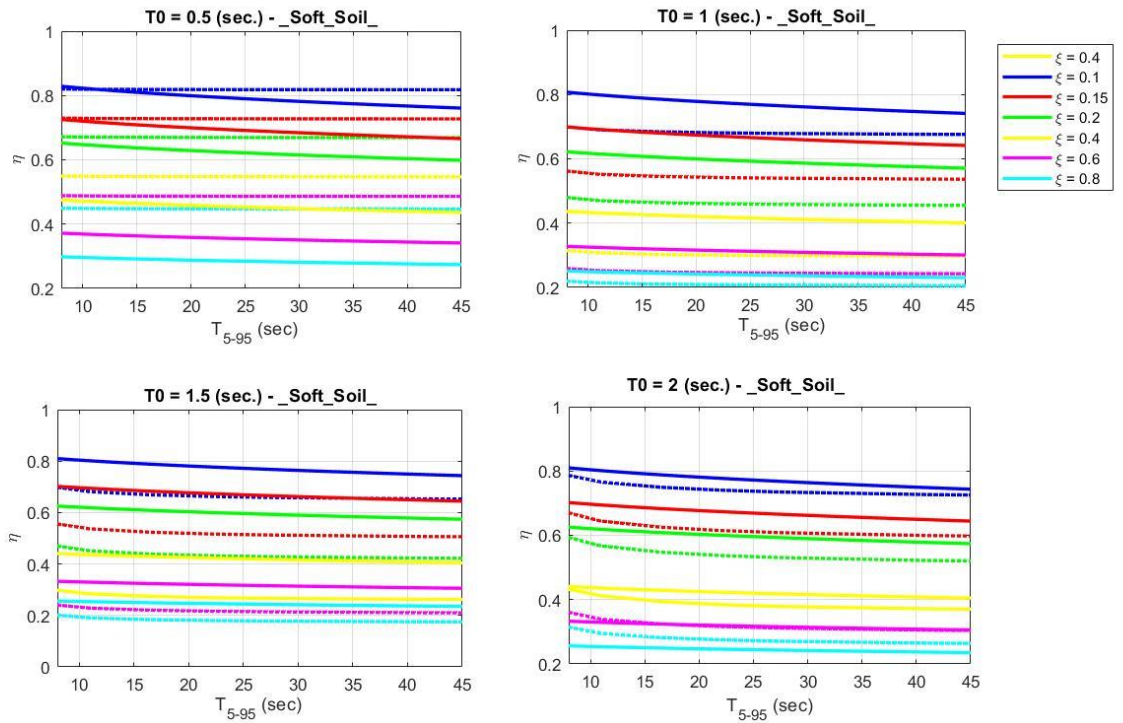


Figure 18 Comparison between proposed formulation (Dashed line) and results in [69] in case of soft soil

480
481
482
483

484
485
486

487 The results obtained from this work have a practical relevance in seismic engineering applications as
488 they allow a more accurate evaluation of the DRF, which accounts also for soil type influence, with
489 respect to other formulation existing in literature, and therefore it furnishes design forces on structures
490 in a more accurate way. One should remind that in practical applications, the effective GMD can be
491 evaluated by existing formulations [70] for a given earthquake scenario that is characterized by
492 parameters such as magnitude, epicentral distance and soil type and therefore the DRF factor can be
493 calculated by proposed formulation for a particular value of damping at any specific period of the
494 structure.

495

496 **7. Conclusions**

497 In this study, a combined evaluation of DRF sensitivity to ground motion duration (GMD), soil type,
498 damping ratio and natural period has been studied; the peak theory of stochastic processes is at the
499 base of the proposed procedure. This theory models the seismic excitation by a non-stationary process
500 characterized by means of a stationary predominant frequency and a given bandwidth. Parameters of
501 modulation function have been identified in order to represent earthquake with different effective
502 durations. The following conclusions can be given on the base of the obtained results. In detail:

- 503 • DRF decreases with the increasing of damping ratio. Moreover, DRF is significantly
504 dependent on the vibration period, reaching a minimum for natural period equal to earthquake
505 predominant period;
- 506 • the effective duration influences DRF: as effective duration increases, DRF decreases.
507 However, this variability is evident in the first part of the effective GMD for reaching the
508 steady state response in the final part. For GMDs larger than 20 s, the DRF tends to an
509 asymptotic final value and there are no significant differences between them (the same result
510 for different GMDs).
- 511 • the variability of DRF with GMD concerns especially deformable systems (in the study $T_0=2$
512 sec is considered) with low damping ratio and becomes negligible for rigid structures ($T_0=2$)
513 with high damping ratio.
- 514 • the variability of DRF with GMD is greater for small damping ratio ($\xi=0.10$) and reduces
515 as the damping ratio increases.
- 516 • DRF depends also on ground type and a larger sensitivity is observed for rigid soil. For
517 example, for this soil the variation of DRF can amount to 0.125 and the implication on
518 practical application can be relevant.

519 Based on conducted stochastic analyses a simple formulation for DRF evaluation, which accounts of
520 effective duration, soil type, damping ratio and natural period of structure has been given. This study
521 gives results with great relevance in structural applications because it emerges that as well as the
522 earthquake GMD must be considered for damage structural evaluation it should be considered also
523 in the evaluation of DRF to avoid an undervaluation of reducing factor of structural seismic forces.
524 This aspect is more relevant for deformable structures on rigid soil and with low damping ratio. The
525 proposed formulation for the DRF, which accounts in addition to the period and the damping also
526 for the effects of the GMD and soil characteristics, results therefore useful for practical applications.
527

528 **8. References**

- 529 [1] Fiorentino, G.; Forte, A.; Pagano, E.; Sabetta, F.; Baggio, C.; Lavorato, D.; Nuti, C.; Santini, S. Damage Patterns
530 in the Town of Amatrice after August 24th 2016 Central Italy Earthquakes. *Bulletin of Earthquake Engineering*
531 2018, 16 (3), 1399–1423.
- 532 [2] Nuti, C.; Santini, S.; Vanzi, I. Damage, Vulnerability and Retrofitting Strategies for the Molise Hospital System
533 Following the 2002 Molise, Italy, Earthquake. *Earthquake Spectra* 2004, 20 (S1), S285–S299.
- 534 [3] Rasulo, A.; Goretti, A.; Nuti, C. Performance of Lifelines During the 2002 Molise, Italy, Earthquake. *Earthquake*
535 *Spectra* 2004, 20 (S1), S301–S314.
- 536 [4] Nuti, C.; Rasulo, A.; Vanzi, I. Seismic assessment of utility systems: Application to water, electric power and
537 transportation networks. *Safety, Reliability and Risk Analysis: Theory, Methods and Applications - Proceedings*
538 *of the Joint ESREL and SRA-Europe Conference*. 2009, 3, 2519-2529.
- 539 [5] Bergami, A. V.; Nuti, C. A Design Procedure of Dissipative Braces for Seismic Upgrading Structures.
540 *Earthquakes and Structures* 2013, 4 (1), 85–108.
- 541 [6] Lavorato, D.; Vanzi, I.; Nuti, C.; Monti, G. Generation of Non-Synchronous Earthquake Signals. *Springer Series*
542 *in Reliability Engineering* 2017; Gardoni, P., Ed.; Springer International Publishing: Cham, 169–198.
- 543 [7] Liu, T., Zordan, T., Zhang, Q., & Briseghella, B. (2015). Equivalent viscous damping of bilinear hysteretic
544 oscillators. *Journal of Structural Engineering*, 141(11), 06015002.
- 545 [8] Lin YY, Miranda E, Chang KC. Evaluation of damping reduction factors for estimating elastic response of
546 structures with high damping. *Earthq Engrg Struct Dyn*. 2005; 34: 1427–43.
- 547 [9] NEHRP. Recommended provisions for seismic regulations for new buildings and other structures. Federal
548 Emergency Management Agency, Washington, DC. 2000.
- 549 [10] UBC. Uniform Building Code. International Conference of Building Officials, Whittier, CA. 1997.

- 550 [11] FEMA-273. NEHRP guidelines for the seismic rehabilitation of buildings. Fed. Emergency Management
551 Agency, Washington DC. 1997.
- 552 [12] IBC. International Building Code. International Conference of Building Officials, Whittier, CA. 2000.
- 553 [13] Fiore A, Marano GC, Natale MG .Theoretical prediction of the dynamic behavior of rolling-ball rubber-layer
554 isolation systems. *Structural Control and Health Monitoring* 2016; 23 (9): 1150-1167.
- 555 [14] Marano GC, Pellicciari M, Cuoghi T, Briseghella B, Lavorato D, Tarantino AM. Degrading bouc-wen model
556 parameters identification under cyclic load *International Journal of Geotechnical Earthquake Engineering*. 2017;
557 8 (2): 60-81.
- 558 [15] Marano GC, Pellicciari M, Cuoghi T, Briseghella B, Lavorato D, Tarantino AM. Parameter identification of
559 degrading and pinched hysteretic systems using a modified Bouc–Wen model. *Structure and Infrastructure*
560 *Engineering*. 2018.
- 561 [16] Bergami AV, Nuti C. A design procedure of dissipative braces for seismic upgrading structures. *Earthquake and*
562 *Structures*. 2013; 4 (1): 85-108.
- 563 [17] Ashour SA. Elastic seismic response of buildings with supplemental damping. Ph.D. Thesis, Department of Civil
564 Engineering, Michigan University. 1987.
- 565 [18] Ramirez OM, Constantinou MC, Whittaker AS, Kircher CA, Chrysostomou CZ. Elastic and inelastic seismic
566 response of buildings with damping systems. *Earthq Spectra*. 2002; 18(3): 531–547.
- 567 [19] Bommer JJ, Elnashai AS, Weir AG. Compatible acceleration and displacement spectra for seismic design codes.
568 In: *Proceedings of the 12th world conference on earthquake engineering*, Auckland. 2000.
- 569 [20] Lin YY and Chang KC. A study on damping reduction factor for buildings under earthquake ground motion.
570 *Journal of the Structural Engineering*. 2003; 129(2): 206–214.
- 571 [21] Lin YY and Chang KC. Effects of site classes on damping reduction factors. *Journal of Structural Engineering*.
572 2004; 130(11): 1667-1675.
- 573 [22] Bommer JJ, Mendis R. Scaling of spectral displacement ordinates with damping ratios. *Earthquake Eng Struct*
574 *Dynam*. 2005; 34:145–65.
- 575 [23] Cameron WI, Green RA. Damping correction factors for horizontal ground motion response spectra. *Bull*
576 *Seismol Soc Am*. 2007; 97(3): 934–60.
- 577 [24] Akkar S, Sandıkkaya MA, Ay BÖ. Compatible ground-motion prediction equations for damping scaling factors
578 and vertical-to-horizontal spectral amplitude ratios for the broader Europe region, *Bulletin of Earthquake*
579 *Engineering*. 2014; 1(12): 517-47.
- 580 [25] Benahemd B, Hamoutenne M, Tiliouine B, Badaoui M. Prediction of the damping reduction factor by neural
581 networks. *Asian Journal of Civil Engineering (BHRC)*. 2016; 17; 225-234.
- 582 [26] Stafford PJ, Mendis R, Bommer JJ. Dependence of damping correction factors for response spectra on duration
583 and numbers of cycles, *J. Struct. Eng*. 2008;8: 1364–1373.

- 584 [27] Rosenblueth E. Characteristics of earthquakes. Rosenblueth E, editor. Design of Earthquake Resistant Structures,
585 Wiley; 1980 [Ch. 1].
- 586 [28] Anbazhagan P, Neaz Sheikh M, Ketan Bajaj, Mariya Dayana PJ, Madhura H, Reddy GR. Empirical models for
587 the prediction of ground motion duration for intraplate earthquakes. *J Seismol.* 2017; 21: 1001.
- 588 [29] Daneshvar P, Bouaanani N, Goda K, Atkinson GM. Damping Reduction Factors for Crustal, Inslab, and Interface
589 Earthquakes Characterizing Seismic Hazard in Southwestern British Columbia, Canada. *Earthquake Spectra.*
590 2016; 32 :45-74.
- 591 [30] Zhou J, Tang K, Wang H, Fang X. Influence of Ground Motion Duration on Damping Reduction Factor. *Journal*
592 *of Earthquake Engineering.* 2014; 18: 816-830.
- 593 [31] Rezaeian S, Bozorgnia Y, Idriss IM, Campbell K, Abrahamson N, Silva W. Damping scaling factors
594 for elastic response spectra for shallow crustal earthquakes in active tectonic regions: Average horizontal
595 component. *Earthquake Spectra.* 2014; 30(2): 939-963
- 596 [32] Greco R, Fiore A, Briseghella B. Influence of soil type on damping reduction factor: A stochastic analysis based
597 on peak theory. *Soil Dynamics and Earthquake Engineering.* 2018; 104: 365-368.
- 598 [33] Greco R, Fiore A, Marano GC. The Role of Modulation Function in Nonstationary Stochastic Earthquake Model.
599 *Journal of Earthquake and Tsunami* 2014; 8(5): 1450015-1-1450015-28.
- 600 [34] Greco R, Marano GC, Fiore A. Performance-cost optimization of Tuned Mass Damper under low-moderate
601 seismic actions. *Structural Design of Tall and Special Buildings.* 2016;25(18), 1103-1122.
- 602 [35] Marano, GC. Envelope process statistics for linear dynamic system subject to nonstationary random vibrations.
603 *Far East Journal of Theoretical Statistics.* 2008; 26; 29 – 46.
- 604 [36] Clough WR, Penzien J. Dynamics of Structures. McGraw-Hill Education (ISE Editions); International 2 Revised
605 edition (dicember 1993); 1977.
- 606 [37] Jennings PC, Housner GW, Tsai NC. Simulated earthquake motions. Technical report, Earthquake Engrng. Res.
607 Lab., California Inst. of Technology; 1968.
- 608 [38] Bommer JJ, Martinez-Pereira A. The effective duration of earthquake strong motion. *Journal of Earthquake*
609 *Engineering.*1999; 3: 127-172.
- 610 [39] Bolt BA. Duration of strong ground motions. Proceedings of the 5th World Conference on Earthquake
611 Engineering, Acapulco.1973.
- 612 [40] Sabetta F. Analisi di quattro definizioni di durata applicate ad accelerogrammi relativi a terremoti italiani. Open
613 File Report, ENEA -RT/AMB 4(83), Roma, Italy. 1983 (Italian).
- 614 [41] Sarma SK, Casey BJ. Duration of strong motion in earthquakes. Proceedings of the 9th European Conference on
615 Earthquake Engineering, Moscow, USSR, 10A. 1990: 174–183.
- 616 [42] Arias, A. A measure of earthquake intensity. In: Hansen RJ, editor. *Seismic Design for Nuclear Power Plants,*
617 *Cambridge, Massachusetts: MIT Press.* 23. 1970: 438-483.

- 618 [43] Trifunac MD, Brady AG. A study on the duration of strong earthquake ground motion. *Bulletin of the*
619 *Seismological Society of America* 65. 1975: 581-626.
- 620 [44] Bommer JJ, Stafford PJ, Alarcon JA. Empirical equations for the prediction of the significant, bracketed, and
621 uniform duration of earthquake ground motion. *Bull Seismol Soc Am* 99(6). 2009: 3217–3233.
- 622 [45] Kempton JJ, Stewart PJ. Prediction equations for significant duration of earthquake ground motions
623 consideration site and near- source effects. *Earthq Spectra* 22. 2006: 958–1013
- 624 [46] Hernandez B, Cotton F. Empirical determination of the ground shaking duration due to an earthquake using
625 strong motion accelerograms for engineering applications. In: *Proceedings, 12th world conference on earthquake*
626 *engineering*. 2000; paper no. 2254/4/A.
- 627 [47] Lutes, LD, Sarkani, S. Failure Analysis. In *Random Vibrations*. London: Butterworth-Heinemann. 2004: 500–
628 570. [Ch 11]
- 629 [48] Marano GC, Acciani G, Fiore A., Abrescia A. Integration algorithm for covariance non-stationary dynamic
630 analysis of SDOF systems using equivalent stochastic linearization. *International Journal of Structural Stability*
631 *and Dynamics* 2015; 15(2): 1450044-1-1450044-17.
- 632 [49] Greco R., Marano GC, Fiore A. Damage-Based Inelastic Seismic Spectra. *International Journal of Structural*
633 *Stability and Dynamics*. 2017; 17(10): 1750115-1-1750115-23.
- 634 [50] Marano GC, Trentadue F., Greco R. Stochastic optimum design criterion of added viscous dampers for buildings
635 seismic protection. *Structural Engineering and Mechanics*. 2007; 25(1): 21-37.
- 636 [51] Greco R, Marano GC. Optimum design of tuned mass dampers by displacement and energy perspectives”, *Soil*
637 *Dynamics and Earthquake Engineering*. 2013; 49: 243-253.
- 638 [52] Lucchini A, Greco R, Marano GC, Monti G. Robust design of tuned mass damper systems for seismic protection
639 of multistory buildings. *Journal of Structural Engineering*. 2014; 140(8): A4014009.
- 640 [53] Greco, R., Lucchini, A., Marano, G.C. Robust design of tuned mass dampers installed on multi-degree-of-
641 freedom structures subjected to seismic action (2015) *Engineering Optimization*, 47 (8), pp. 1009-1030.
- 642 [54] Marano, G.C., Trentadue, F., Greco, R. Optimum design criteria for elastic structures subject to random dynamic
643 loads (2006) *Engineering Optimization*, 38 (7), pp. 853-871.
- 644 [55] Vanzi I, Marano GC, Monti G, Nuti C. A synthetic formulation for the Italian seismic hazard and code
645 implications for the seismic risk *Soil Dynamics and Earthquake Engineering*. 2015;77: 111-122.
- 646 [56] Bergami AV, Forte A, Lavorato D, Nuti C. Proposal of a Incremental Modal Pushover Analysis (IMPA).
647 *Earthquake and Structures*. 2017; 13 (6): 539-549.
- 648 [57] Fiorentino G, Forte A, Pagano E, Sabetta F, Baggio C, Lavorato D, Nuti C, Santini S. Damage patterns in the
649 town of Amatrice after August 24th 2016 Central Italy earthquakes. *Bulletin of Earthquake Engineering*. 2017:
650 1-25.
- 651 [58] Resta M, Fiore A, Monaco P. Non-Linear Finite Element Analysis of Masonry Towers by Adopting the Damage
652 Plasticity Constitutive Model”, *Advances in Structural Engineering*. 2013; 16(5): 791-803.

- 653 [59] Fiore A, Monaco P. Earthquake-induced pounding between the main buildings of the “Quinto Orazio Flacco”
654 school. *Earthquakes and Structures*. 2010; 1(4): 371-390.
- 655 [60] Fiore A., Spagnoletti G., Greco R., On the prediction of shear brittle collapse mechanisms due to the infill-frame
656 interaction in RC buildings under pushover analysis. *Engineering Structures* 2016; 121: 147-159.
- 657 [61] Colapietro, D., Fiore, A., Netti, A., Fatiguso, F., Marano, G.C., De Fino, M., Cascella, D., Ancona, A., 2013.
658 Dynamic identification and evaluation of the seismic safety of a masonry bell tower in the south of Italy.
659 ECCOMAS Thematic Conference - COMPDYN 2013: 4th International Conference on Computational Methods
660 in Structural Dynamics and Earthquake Engineering, Proceedings - An IACM Special Interest Conference 2013;
661 3459-3470.
- 662 [62] Greco R, Marano GC. Site based stochastic seismic spectra. *Soil Dynamics and Earthquake Engineering*. 2013:
663 288-295.
- 664 [63] Vanmarcke EH, Gasparini DA. Compatible Simulated earthquake motions with prescribed answer will spectra.
665 SIMQKE User' S manual and documentation. MIT R76-4 Carryforward. 1976.
- 666 [64] Rice SO. Mathematical analysis of random noise. *Bell Syst. Tech. J.*, 23(3). 1994: 282–332.
- 667 [65] Atkinson GM, Pierre JR. Ground-motion Response Spectra in Eastern North America for Different Critical
668 Damping Values. *Seismological Research Letters*. 2004; 75(4): 541-545.
- 669 [66] Stafford PJ, Mendis R, Bommer JJ. Dependence of damping correction factors for response spectra on duration
670 and numbers of cycles. *ASCE, J Struct Engrg*. 2008; 134: 1364–73.
- 671 [67] MATLAB and Statistics Toolbox Release 2012b, The MathWorks, Inc., Natick, Massachusetts, United States.
- 672 [68] Quaranta G, Fiore A, Marano GC. Optimum design of prestressed concrete beams using constrained differential
673 evolution algorithm. *Structural and Multidisciplinary Optimization* 2014; 49(3): 441–453.
- 674 [69] Shih-Sheng PL. Statistical characterization of strong ground motions using power spectral density function.
675 *Bulletin of the Seismological Society of America* 72(1). 1982: 259-274.
- 676 [70] Mohraz B. *The Seismic Design Handbook- Chapter 2 Earthquake Ground Motion and Response Spectra*.
677 Springer Science & Business Media. 2012.
- 678